J Mater Sci (2010) 45:4827–4836
DOI 10.1007/s10853-010-4589-y

ULTRAFINE GRAINED MATERIALS

Grain refinement and mechanical behavior of a magnesium alloy processed by ECAP

Roberto B. Figueiredo · Terence G. Langdon

Received: 23 January 2010 / Accepted: 30 April 2010 / Published online: 14 May 2010

Abstract Equal-channel angular pressing (ECAP) is an effective tool for refining the grain structure of magnesium alloys and improving the ductility at moderate temperatures. However, grain refinement in these alloys differs from other metals because new grains are formed along the boundaries of the initial structure and these newly formed grains slowly spread to consume the interiors of the larger grains in subsequent passes. A model is presented for grain refinement in magnesium alloys processed by ECAP based on the principles of dynamic recrystallization where new fine grains are formed along the initial boundaries and along twin boundaries. This model provides an explanation for a wide range of experimental data and introduces the concept of grain size engineering for achieving selected material properties in magnesium alloys.

Introduction

Magnesium and its alloys are attractive light metals due to their high strength per weight ratio. Nevertheless, there has been only a limited use of magnesium alloys in industrial applications because of their low formability at low temperatures and the consequent difficulties often encountered in the shaping of components. An important consequence of this limitation is that the processing of magnesium alloys is generally conducted at moderate or high temperatures. The thermo-mechanical processing of magnesium alloys leads to changes in the structure of the material and specifically to changes in the grain size and in the grain size distribution. Typical cast structures are characterized by coarse grains of several hundreds of microns, whereas wrought materials, processed by hot extrusion or rolling, usually exhibit a heterogeneous distribution of fine and coarse grains. This multi-modal distribution of grain sizes in wrought magnesium is a direct consequence of the formation by dynamic recrystallization of fine grains along the grain boundaries when processing at moderate temperatures. In practice, however, the total deformation achieved by conventional thermo-mechanical processing is severely limited by the concomitant reduction in the cross-sectional areas of the samples. As a result, this type of processing is usually not sufficient to promote a homogeneous refinement of the initial coarse structure of the material and it leads instead to a multi-modal grain size distribution.

Over the last two decades, the development of processing techniques incorporating the application of severe plastic deformation (SPD), as in equal-channel angular pressing (ECAP) [1], eliminated the constraint on the amount of deformation that may be imposed on a material during processing. Thus, the introduction of SPD techniques for the processing of magnesium alloys gave the possibility of producing materials having homogeneous arrays of ultrafine grains with improved mechanical properties including exceptional superplastic capabilities.

In practice, it became clear during this period that the mechanism of grain refinement in magnesium alloys processed by ECAP differs in a significant way from the mechanism observed in f.c.c. metals such as aluminum and copper. In the f.c.c. metals, the first pass of ECAP produces an array of elongated subgrains oriented with their longer

R. B. Figueiredo · T. G. Langdon
Materials Research Group, School of Engineering Sciences, University of Southampton, Southampton SO17 1BJ, UK

T. G. Langdon (✉)
Departments of Aerospace & Mechanical Engineering and Materials Science, University of Southern California, Los Angeles, CA 90089-1453, USA
e-mail: langdon@usc.edu

axes aligned parallel to the primary slip system and with the boundaries having low angles of misorientation [2, 3]. Additional passes introduce additional dislocations and these dislocations re-arrange and annihilate consistent with the low-energy dislocation structures theory [4, 5] to give, typically after about four passes of ECAP, an array of reasonably equiaxed grains separated by boundaries having high angles of misorientation. The evolution of this structure has been documented in detail in several f.c.c. materials including high-purity aluminum [6]. By contrast, in magnesium and its alloys the new ultrafine grains produced by ECAP form along the original boundaries so that the initial large grains are ultimately consumed by these new smaller grains as the number of ECAP passes increases.

The nature of this mechanism of grain refinement in magnesium alloys is dependent upon the initial grain structure prior to ECAP and various parameters involved in the ECAP processing. As a result of the various possible structural and processing permutations, it follows that diverse microstructural features have been reported for these materials after processing by ECAP including different final grain sizes and various multi-modal distributions of grain sizes. The present research was undertaken to examine the microstructures and the mechanical properties of an AZ31 magnesium alloy processed by ECAP and to develop a comprehensive model for grain refinement that may be used for the processing of magnesium-based alloys by ECAP. As will be demonstrated, the model described for grain refinement leads to a general understanding of the various reports appearing in the literature and it provides a predictive capability for anticipating the new grain structures that will be produced in magnesium alloys under different experimental conditions. The model is based on, and represents an extension of, an earlier simple model describing grain refinement in magnesium alloys [7]. It is important to emphasize, however, that the detailed mechanism of grain refinement developed in this report permits the formation of different structures depending upon the processing conditions and, in addition, it has direct implications concerning the optimum processing routes for the successful processing of these materials.

Experimental material and procedures

An AZ31 magnesium alloy (Mg–3 wt% Al–1 wt% Zn) was received in the form of extruded rods with diameters of $\sim$10 mm. These rods were cut into 60-mm long billets and processed by ECAP in the as-received condition. The ECAP was carried out at a temperature of 473 K using a solid die with an angle of 110° between the channels and an external arc of curvature of 20° to give an imposed strain of $\sim$0.8 in each separate pass [8]. The billets were pressed for up to six passes with a punch speed of $\sim$7 mm s^{-1} using route B_C in which each billet is rotated by 90° in the same sense between passes [9]. Earlier reports provided additional information on the processing of the AZ31 alloy by ECAP [10, 11].

The grain structure was evaluated before and after ECAP using conventional metallographic techniques. Samples were cut from the billets and cold mounted in resin. The cross sections of the billets were ground, polished, and etched using an acetic-picral solution. The etched samples were observed using optical microscopy and the grain sizes were determined for each sample as the mean linear intercept grain size.

Tensile specimens with gauge lengths of 4 mm and cross-sectional areas of 3×2 mm^2 were machined from the as-received rods and the billets processed through six passes of ECAP. These tensile specimens were tested in the temperature range from 423 to 473 K using an Instron testing machine operating at a constant rate of crosshead displacement with initial strain rates in the range from 3.3×10^{-5} to 3.3×10^{-3} s^{-1}.

Experimental results

Grain structure

Representative photo-micrographs of the grain structures are shown in Fig. 1 for (a) the as-received material before ECAP, (b) the material after two passes of ECAP, and (c)

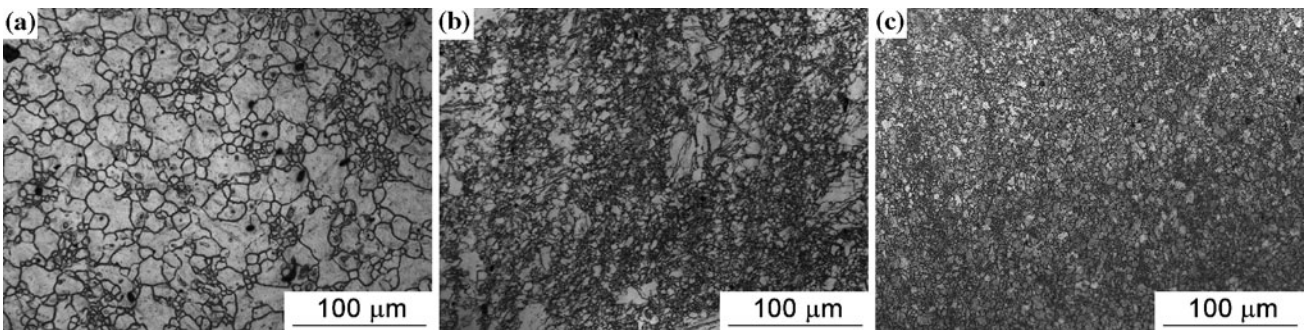

Fig. 1 Grain structure of the AZ31 magnesium alloy in **a** the initial as-received condition and after **b** two and **c** six passes of ECAP

the material after six passes of ECAP, respectively. It is apparent from Fig. 1a that the as-received material exhibits a broad distribution of grain sizes from a few microns to tens of microns. Measurements gave an average grain size in this condition of ~9.4 μm. The grain structure after processing by two passes, shown in Fig. 1b, also contains a broad distribution of grain sizes but the area fraction of small grains of only a few microns has now increased and the area fraction of the coarser grains has been significantly reduced. Furthermore, some of the larger grains of a few tens of microns are now visibly distorted and surrounded by much finer grains. For this condition, the measured average grain size was ~2.5 μm. After six passes in Fig. 1c the coarse grains have been removed and instead the cross section of the billet is filled with very fine grains. For this condition, the average grain size was ~1.6 μm. These observations demonstrate that six passes of ECAP are sufficient to produce a homogeneous grain structure in the AZ31 alloy.

Mechanical properties at moderate temperatures

Tensile tests were carried out on the as-received material at different strain rates at 423 and 473 K. The true stress–true strain curves for the as-received material are given in Fig. 2. Inspection shows that the flow stress decreases both with an increasing testing temperature and with a decreasing strain rate. Furthermore, the material exhibits hardening in the initial stages of deformation and this effect is more pronounced at the lowest temperature and highest strain rate. After the hardening stage, the material exhibits a continuous decrease in the flow stress up to failure where this is attributed to necking during the tensile deformation.

Tensile tests were also conducted on the material processed through six passes of ECAP at the intermediate strain rate of 3.3×10^{-4} s^{-1} and at the temperatures of

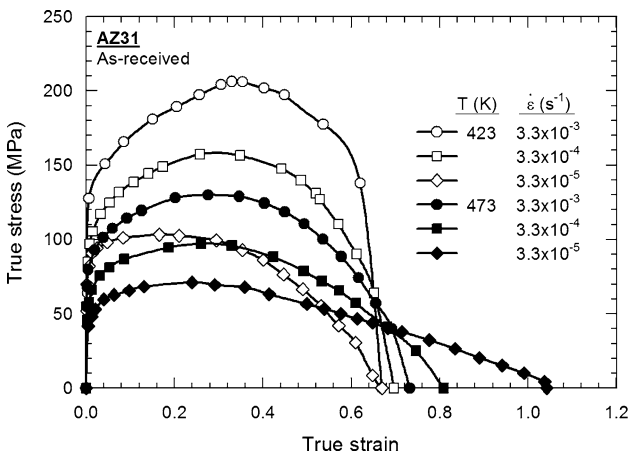

Fig. 2 True stress versus true strain for tests at 423 and 473 K on the as-received AZ31 alloy

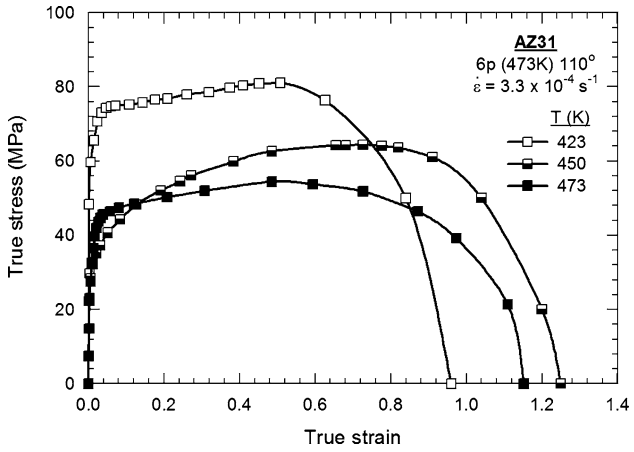

Fig. 3 True stress versus true strain for tests at 423, 450, and 473 K on the AZ31 alloy processed through six passes of ECAP

423, 450, and 473 K. These results are shown in Fig. 3 where it is apparent that the yield stress decreases from 423 to 450 K but thereafter increases slightly from 450 to 473 K. This is analogous to results reported earlier for a ZK60 magnesium alloy, also pressed by ECAP at 473 K, where there was a decrease in the strain rate sensitivity and in the measured elongations to failure at a testing temperature of 493 K due, it was suggested, to an instability in the ultrafine microstructure at temperatures at or above the pressing temperature of 473 K [12].

A direct comparison of Figs. 2 and 3 shows also that there is a decrease in the flow stress of the material processed by ECAP compared to the as-received material. This difference in flow stress is attributed to texture effects as ECAP leads to a favorable orientation of the basal planes for tensile deformation. A reduction of the flow stress after ECAP compared to the extruded condition was observed also in a similar alloy at 523 K [13]. It has been reported that the effect of texture on the flow stress of a magnesium alloy decreases and ultimately disappears when the temperature is raised from 573 to 648 K [14].

Additional tests were conducted on the material pressed through six passes using different strain rates and a constant temperature of 450 K. The results are shown in Fig. 4 where it is apparent that the flow stress decreases with decreasing strain rate. Contrary to the results observed with the as-received material, the extent of the hardening in Fig. 4 increases with decreasing strain rate so that the peak stresses occur at strains of ~0.5, ~0.7, and ~0.8 at strain rates of 3.3×10^{-3}, 3.3×10^{-4}, and 3.3×10^{-5}, respectively.

The strain rate sensitivity, m, was determined by cyclically changing the strain rate during the tests. The results are summarized in Table 1 together with the values of the elongations to failure for all tests conducted on the

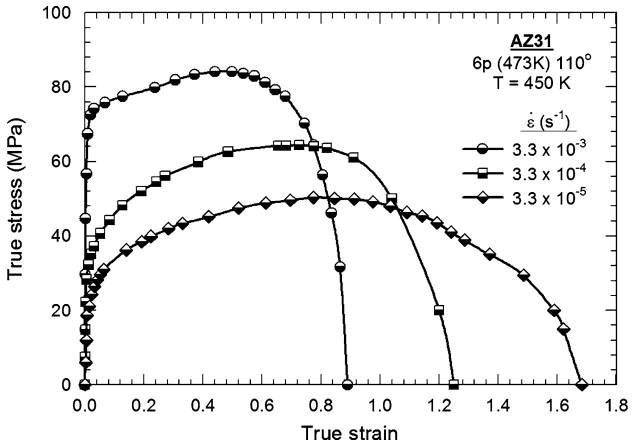

Fig. 4 True stress versus true strain for tests at different strain rates at 450 K on the AZ31 alloy processed through six passes of ECAP

Table 1 Strain rate sensitivities and elongations in tensile testing

Temperature (K)	Strain rate (s^{-1})	Strain rate sensitivity, m	Elongation (%)
As-received			
423	3.3×10^{-5}	0.17	95
	3.3×10^{-4}	0.10	100
	3.3×10^{-3}	0.01	95
473	3.3×10^{-5}	0.26	185
	3.3×10^{-4}	0.17	125
	3.3×10^{-3}	0.11	110
ECAP: six passes (473 K) 110°			
423	3.3×10^{-4}	0.12	160
450	3.3×10^{-5}	0.32	430
	3.3×10^{-4}	0.31	250
	3.3×10^{-3}	0.09	130
473	3.3×10^{-4}	0.16	210

as-received material and after processing through six passes of ECAP. All values of m are relatively low but higher values were recorded at a temperature of 450 K in the material processed by ECAP. As anticipated, these higher values of m lead to larger elongations prior to failure. For the present tests, a maximum elongation of 430% was recorded in the material processed by ECAP when testing at 450 K at the lowest strain rate of 3.3×10^{-5} s^{-1}. This elongation is above the limiting value of 400% which delineates the onset of superplastic flow [15] although the strain rate sensitivity of 0.32 is low by comparison with conventional superplasticity where, typically, $m \approx 0.5$. The elongation is also low by comparison with earlier reports of elongations of >1000% for the AZ31 alloy processed by ECAP and tested at the higher temperatures of 623 and 673 K, respectively [10, 16].

Discussion

The preceding results show that the AZ31 magnesium alloy may be successfully processed by ECAP at a temperature of 473 K. A homogeneous microstructure is produced after six passes of ECAP, as shown in Fig. 1c, and the alloy displays improved ductilities at elevated temperatures including evidence for the onset of superplastic flow when testing in tension at 450 K. However, it is not feasible to make use of the grain refinement model developed earlier for f.c.c. metals where new grains are formed through an evolution of the dislocation structure [3] because this cannot account for either a bi-modal grain distribution or the development of a heterogeneous distribution of grain sizes. It is necessary instead to consider a process of grain refinement based on dynamic recrystallization.

Formation of fine grains along the grain boundaries by dynamic recrystallization

Early studies showed the occurrence of dynamic recrystallization in magnesium alloys deformed in the temperature range of ~420–600 K [17–20] where this corresponds to the temperature range often used for the processing of magnesium alloys by ECAP. In dynamic recrystallization, the grains nucleate preferentially along the original boundaries of the coarse-grained structure and along twin boundaries in a necklace-like pattern so that the inner cores of the coarse grains may not be refined. An early model for the nucleation of grains along grain boundaries by dynamic recrystallization was based on the anisotropy of the shear stresses needed to activate slip on different systems in the h.c.p. structure [18]. It is anticipated that only systems having easy slip will be activated in the cores of the grains and this will be insufficient to successfully produce grain refinement. In practice, the stresses are higher at the grain boundaries because of the incompatibilities in slip between the neighboring grains and these higher stresses activate the harder slip systems and promote the formation of three-dimensional arrays of dislocations thereby triggering dynamic recrystallization in these areas [18]. It follows, therefore, that the grain refinement of magnesium alloys is dependent upon the numbers of sites available for the nucleation of new grains.

The nucleation of fine grains along the grain boundaries of coarse-grained structures during ECAP has been observed directly using transmission electron microscopy (TEM) [21], electron back-scatter diffraction [21, 22], and optical microscopy [7, 11]. In addition, there are reports in ECAP of subgrain structures in the cores of the coarse grains [21, 23] but with fine grains separated by high-angle grain boundaries formed along the traces of the original boundaries. These observations confirm that the fundamental mechanism for the nucleation of fine grains along

grain boundaries and twin boundaries by dynamic recrystallization is applicable also in the processing of magnesium alloys by ECAP.

Any viable model for the grain refinement of magnesium alloys in ECAP must incorporate these fundamental aspects of dynamic recrystallization. In practice, however, any model must also consider the size of the initial coarse grains and the size of the grains produced during grain refinement. These two conditions are examined in the following sections and the next sections outline a model to describe grain refinement in magnesium during ECAP.

The effect of the initial coarse grain size

The nucleation of fine grains in magnesium alloys, when deformed in the temperature range ~420–600 K as in ECAP, takes place along the grain and twin boundaries due to the higher stresses that are then present to activate the harder slip systems. The activation of these harder slip systems in magnesium alloys becomes easier at higher temperatures but, in addition, it depends also on the grain size. In tests on an AZ31 alloy with a grain size of only ~6.5 μm, observations by TEM showed that non-basal slip became activated at room temperature at stresses similar to those required for basal slip and the results were attributed to an easier compatibility between the individual small grains [24]. This result has implications for ECAP because it means that the activation of non-basal slip, and consequently the nucleation of fine grains by dynamic recrystallization, should be easier when conducting the ECAP either at a higher processing temperature and/or when using a material with an exceptionally small initial grain size.

The size of the fine grains formed by dynamic recrystallization

Another important parameter in the processing of magnesium alloys by ECAP is the size of the grains formed by dynamic recrystallization. Experiments on an AZ31 alloy showed that the size of the fine grains produced during ECAP was dependent upon the speed of processing and the pressing temperature with the results following a general Zener–Hollomon relationship [21]. For practical situations, however, it is reasonable to anticipate that finer grains will be produced when processing at lower temperatures and/or faster speeds.

An examination of published reports of microstructures produced in Mg and magnesium alloys by ECAP

In order to develop a satisfactory model, it is first necessary to review the various grain structures reported in the literature for the processing of magnesium alloys by ECAP. An earlier report tabulated some of these experimental data [25] but a more comprehensive summary is given in Table 2 for experiments conducted on pure magnesium and a range of magnesium alloys [11, 16, 21–23, 26–48]. Except where indicated otherwise, the results in Table 2 refer to the use of an ECAP die with an internal channel angle of 90°, processing by route B_C and pressing without a back-pressure: exceptions are marked in the sixth column of Table 2 where Φ is the channel angle within the die, BP denotes the use of a back-pressure and routes A, B_A, and C refer to processing without rotation of the specimen between passes, with a rotation of 90° in alternate directions between passes and with a rotation of 180° between passes, respectively. The first column in Table 2 lists the material, the second and third columns give the initial and final grain sizes, respectively, the fourth and fifth columns describe the structure at an intermediate stage of processing and after multiple passes of ECAP, and the last column gives the reference. For additional ease of examination, grain structures after ECAP are also marked with the notation Bi-m or Tri-m to denote reports of bi-modal or tri-modal grain size distributions, respectively.

Inspection of Table 2 shows that heterogeneous grain size distributions are observed after multiple passes only when the initial grain size is large: specifically, heterogeneous grain sizes were reported when the initial grain sizes were in the range from a minimum of 45.5 μm for a ZK60 alloy [46, 47] to a maximum of 640 μm for an AZ31 alloy [16]. The available evidence suggests that grain sizes below ~40 μm are sufficiently small to achieve a homogeneous array of grains by ECAP provided the processing is continued through a reasonable number of passes. Conversely, homogenization is achieved more readily at higher temperatures: for example, although there was a bi-modal grain size in the AZ31 alloy after six passes at 423 K, a homogeneous structure was achieved in the same alloy after six passes at 473 K [16]. A bi-modal grain size was also observed in an Mg–Zn–Y–Zr alloy having an initial mix of coarse and fine grains [43].

Two important criteria emerge from inspection of Table 2. First, a bi-modal grain size distribution is favored when the initial grain size is large or when the initial material contains at least a reasonable fraction of coarse grains. Second, the tabulation of results demonstrates that the same initial structure may evolve to a bi-modal or a tri-modal grain size distribution or to a homogeneous distribution depending upon the processing parameters.

A model for grain refinement in Mg and magnesium alloys processed by ECAP

Figure 5 gives a schematic illustration of a comprehensive model for structural evolution during the processing of

Table 2 Grain structures produced in pure magnesium and magnesium alloys using ECAP

Alloy	Initial grain size (μm)	Final grain size (μm)	Intermediate structure	Structure after multiple passes	Additional information	References
AZ31	48.3	2.5	Heterogeneous	Homogeneous	1st pass at 593 K/last pass at 473 K	Kim and Kim [26]
AZ31	48.1	1.4	Homogeneous	Homogeneous	$\Phi = 100°$	Su et al. [27]
AZ31	2.5	0.7	–	Homogeneous	$\Phi = 110°$	Lin et al. [28]
AZ31	15–22	1	Heterogeneous after four passes	Homogeneous after eight passes	BP-ECAP (423 K)	Xia et al. [29]
AZ31	15–22	2	Homogeneous after four passes	Homogeneous after eight passes	(473 K)	Xia et al. [29]
AZ31	5–30	1.9	Heterogeneous	Homogeneous	Pre-deformed by extrusion	Jin et al. [30]
AZ31	5–30	2.2	Heterogeneous	Homogeneous	$\Phi = 110°$	Figueiredo and Langdon [11]
AZ31	450	1–3 (coarse)/0.5–0.8 (fine)	Heterogeneous	Heterogeneous		Janeček et al. [23]
AZ31	20	1–2	–	Homogeneous	Pre-deformed by hot-rolling	Zúberová et al. [31]
AZ31	10–20	3.0	Heterogeneous	Homogeneous		Estrin et al. [22]
AZ31	10	3.2	–	Homogeneous	Pre-deformed by rolling	Lapovok et al. [16]
AZ31	640	2.5	–	Homogeneous	BP-ECAP (473 K)	Lapovok et al. [16]
AZ31	640	16.5 (coarse)/0.5 (fine)	–	Heterogeneous (Bi-m)	BP-ECAP (423 K)	Lapovok et al. [16]
AZ31	223	Tens of microns (coarse)/ ~3 (fine)	Heterogeneous	Heterogeneous	First four passes at 673 K and last pass at 523 K	Kang et al. [32]
AZ31	~7 (some coarse grains >20)	~2	Heterogeneous	Homogeneous	Route A	Ding et al. [21]
AZ31	15–22	0.9	Heterogeneous	Homogeneous	BP-ECAP	Xu et al. [33]
AZ31	28	8	Heterogeneous	–	One pass of BP-ECAP	Kang et al. [34]
AZ61	16	0.62	Homogeneous	Homogeneous	Pre-deformed by extrusion	Miyahara et al. [35]
AZ91		0.5	–	Homogeneous	Pre-deformed by extrusion	Mabuchi et al. [36]
AZ91	40	1.2	Heterogeneous	Homogeneous	Route C	Máthis et al. [37]
AZ91		0.5		Homogeneous	Route B_A First pass at 538 K/last pass at 423 K	Mussi et al. [38]
AZ91	Tens of microns (coarse)/15 (fine)	2	Heterogeneous	Homogeneous	Pre-deformed by hot-rolling	Chen et al. [39]
Mg (pure)	400	~120	–	Homogeneous		Yamashita et al. [40]
Mg (pure)	200	20 (coarse)/6–8 (fine)	Heterogeneous	Heterogeneous		Suwas et al. [41]
Mg (pure)	900	70	Heterogeneous	Homogeneous		Gan et al. [42]
Mg–0.9% Al	100	17	–	Homogeneous		Yamashita et al. [40]
Mg–6.43% Zn–1.0% Y–0.48% Zr	Coarse >100/fine ~10	Tens of microns (coarse)/ ~1 (fine)	Heterogeneous (Bi-m)	–	One pass	Tang et al. [43]

Table 2 continued

Alloy	Initial grain size (μm)	Final grain size (μm)	Intermediate structure	Structure after multiple passes	Additional information	References
Mg–9% Al	12	0.7	–	Homogeneous (two passes at 473 K)	Pre-deformed by extrusion	Matsubara et al. [44]
ZE41A	80	1.5	Heterogeneous up to 16 passes	Homogeneous after 32 passes	Rotary-die ECAP	Ma et al. [45]
ZK60	45.5	26.7 (coarse)/2 (fine)	Heterogeneous (Bi-m)	Heterogeneous (Bi-m)	$\Phi = 120°$ Route A	Lapovok et al. [46]
ZK60	45.5	19.3 (coarse)/2 (fine)	Heterogeneous (Bi-m)	Heterogeneous (Bi-m)		Lapovok et al. [46]
ZK60	45.5	12.5 (coarse)/4 (intermediate)/0.4 (fine)	–	Heterogeneous (Tri-m)		Lapovok et al. [47]
ZK60	5	1.4	–	Homogeneous	Pre-deformed by extrusion	Watanabe et al. [48]
ZK60	2–15	0.8	Homogeneous	Homogeneous		Figueiredo and Langdon [11]
ZK60	180	~10 (coarse)/~ 1 (fine)	Heterogeneous	Heterogeneous (Bi-m)	$\Phi = 110°$	Figueiredo and Langdon [11]

magnesium alloys by ECAP. This model is developed from a simpler mechanism proposed earlier [7] and it incorporates specific predictions based on the nature of the initial grain size distribution.

The left column of Fig. 5, given by Fig. 5a, d, g, and j, illustrates different initial structures prior to ECAP and incorporates the concept of a critical grain size, d_c, which is sufficiently small that it leads to homogeneous nucleation throughout the original grains when processing. Specifically, Fig. 5a denotes a coarse initial structure with an average grain size, d, which is much larger than the critical size so that $d \gg d_c$, Fig. 5d, g denotes coarse initial structures with $d > d_c$ and Fig. 5j denotes an initial structure finer than the critical size so that $d < d_c$. In practice, the critical size for homogeneous nucleation is associated with the grain size at which non-basal slip is activated throughout the grains. Although further studies are now needed to accurately quantify this parameter, it is reasonable to anticipate that it will depend on the specific alloy and processing

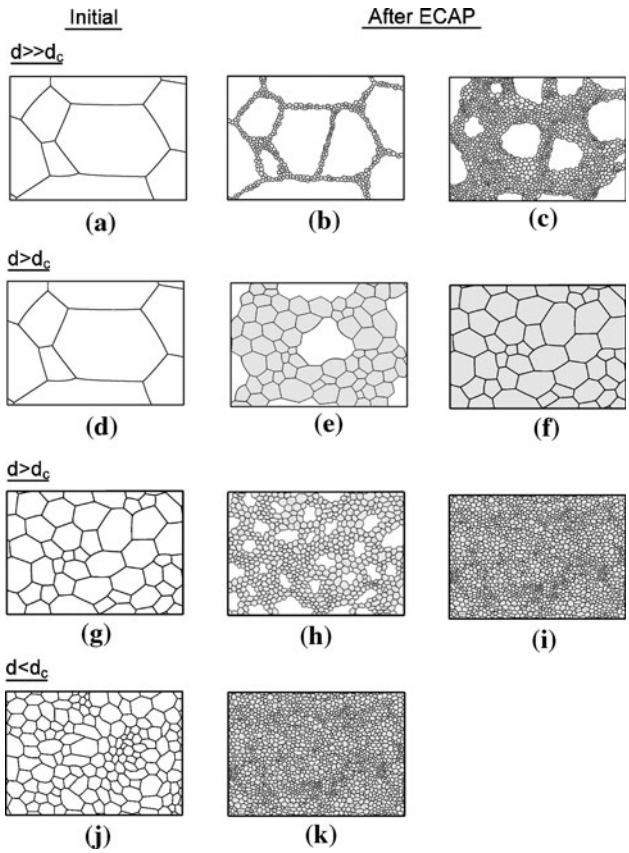

Fig. 5 A model for the grain refinement of magnesium alloys processed by ECAP: the *left column* shows the initial condition, the *second column* shows the structure after one pass and the *third column* shows the structure after multiple passes; the *upper two rows* show the same initial structure with different processing parameters and the *third and fourth rows* show different initial structures

temperature and there is also recent experimental evidence that it depends on the presence of a back-pressure [34].

The second column in Fig. 5 denotes the structure after a single pass of ECAP and the third column denotes the structure after multiple passes. Whenever the initial grain size is larger than d_c, as in Fig. 5a, d, and g, the structure evolves in the first pass into a bi-modal or multi-modal grain distribution as illustrated in Fig. 5b, e, and h. It follows from an examination of the second column in Fig. 5 that the area fractions occupied by the large cores of the initial grains and the area fractions occupied by the new refined grains are critically dependent upon the size of the initial grains. In order to clearly differentiate between the cores of the initial larger grains which remain present after the first pass of ECAP, these core areas are shown in white in the illustrations in the second and third columns, whereas the newly formed refined grains are highlighted in gray.

The upper row in Fig. 5 shows the situation where the initial structure is exceptionally coarse so that the areas of the cores of the larger initial grains continue to occupy a large fraction of the structure after a single pass in Fig. 5b and they also occupy a significant fraction after multiple passes in Fig. 5c. Figure 5b includes also an example where twinning across a large grain has led to grain refinement along the twin. The situation where $d \gg d_c$ leads directly to a bi-modal or multi-modal grain size distribution that persists through many passes of ECAP as illustrated in Fig. 5c.

The size of the newly formed grains also plays a key role in determining whether there is ultimately a homogeneous or multi-modal grain size distribution. In Fig. 5a, d, the initial grain structure is identical but the processing parameters, such as the pressing temperature, have different values for d_c and this leads to different sizes for the newly formed grains. In the first row of Fig. 5, the initial structure is too coarse compared to the size of the newly formed grains so that the volume fraction of these new grains is small after a single pass and this leads to a bi-modal or multi-modal grain size distribution after multiple passes. In the second row, the same initial structure is processed under different conditions, such as at a higher temperature and/or lower strain rate, and this leads to newly formed grains that are larger in size and occupy a larger volume fraction after one pass as shown in Fig. 5e and to a homogeneous structure after multiple passes as shown in Fig. 5f.

In the third row, Fig. 5g illustrates the situation where the initial structure is reasonably fine but the grains are sufficiently coarse that a bi-modal or multi-modal grain size distribution develops after one pass of ECAP but with an area fraction of newly formed grains that is larger than the area occupied by the remaining cores of the initial grains. Further refinement occurs in subsequent passes to give a homogeneous distribution of very fine grains after multiple passes as shown in Fig. 5i.

Finally, when there is a small initial grain size and $d < d_c$ as in Fig. 5j, it is possible to produce a homogeneous array of fine grains in the first pass as illustrated in Fig. 5k and this structure remains homogeneous in subsequent passes.

The important conclusion from this model is that the bi-modal or multi-modal grain size distributions often reported after ECAP are transitional in nature and may be removed, or at least significantly changed, if the pressing is continued through a sufficiently large number of passes.

A comparison of the model with experimental results

The AZ31 alloy used in this investigation was received in the form of extruded rods. As a consequence of this thermo-mechanical processing, the grain structure before ECAP exhibited a heterogeneous distribution of grain sizes ranging from a few microns to tens of microns as shown in Fig. 1a. As some of the grains were exceptionally coarse, the structure should evolve according to the model shown in the second and third rows of Fig. 5 thereby producing a bi-modal or multi-modal grain size distribution in the early stages of processing. This is confirmed in Fig. 1b where some coarse unrefined grains are present after two passes of ECAP. Since the area fraction occupied by the new fine grains is larger than the area of the coarse grains, further processing leads to a homogeneous refinement as shown in Fig. 1c after six passes. These experimental results are therefore consistent with the model in Fig. 5.

Experiments have shown that it is possible to achieve different grain structures from the same initial material by changing the ECAP processing parameters [29]. Using an AZ31 alloy with an initial structure having grain sizes as large as $\sim$22 μm, it was shown that a bi-modal grain size distribution evolves when processing by ECAP at 423 K, whereas a homogeneous grain size distribution is achieved when processing at 473 K. These results are consistent with the models shown in the first and second rows of Fig. 5, respectively. Thus, the newly formed grains are too small compared to the initial grains when processing at the lower temperature but an increase in temperature gives larger new grains and an easier removal of the initial coarse structure.

It was shown earlier that the same processing parameters may lead to different structures depending on the nature of the initial material [11]. Thus, experiments on ZK60 alloys with initial average grain sizes of $\sim$100 and $\sim$3 μm led to the formation of a multi-modal distribution of grain sizes in the former and a homogeneous distribution of ultrafine grains in the latter. These results are consistent with the model evolutions shown in the first and fourth rows of Fig. 5, respectively.

Successful processing routes for ECAP with magnesium alloys

The mechanism of grain refinement in magnesium alloys during ECAP affects the selection of the processing route not only because it influences the final structure but also because of the effect on shear localization and billet failure. It has been shown that deformation may concentrate along a thin layer of the new grains formed along the original grain boundaries and this leads to the formation of shear bands [17]. This concentration of shear in a layer occurs at the expense of shear within neighboring areas and may lead to billet failure due to the increase in damage accumulation [49]. The amount of shear in a shear band increases in coarse structures because of the increase in volume of the cores of the initial grains. This means that the susceptibility to shear localization is high for the sequence shown in the top line of Fig. 5, intermediate for the second and third lines and low for the fourth line. This conclusion is in agreement with experimental results documenting the failure of coarse-grained magnesium alloys [11, 49].

Processing routes have been developed for magnesium alloys specifically to overcome these difficulties including introducing a prior step of extrusion before ECAP in the EX-ECAP process [44, 50], increasing the processing temperature [40], increasing the die angle [51, 52], and using a back-pressure [29]. A preliminary step of extrusion refines the microstructure, reduces the ratio between the grain cores and the boundary volumes, and thereby reduces the tendency for shear localization. Thus, an extrusion step changes the initial structure from the condition shown in Fig. 5a to the conditions shown in Fig. 5g or j. An increase in the processing temperature increases the size of the newly formed grains and changes the refinement sequence from the first to the second rows in Fig. 5. This introduces a larger volume of new grains and a lower tendency for shear localization. An increase in the ECAP die angle also reduces the amount of strain introduced in each separate pass and this reduces the strain in the shear bands and the consequent amount of damage accumulation. Experimental evidence has shown that the use of a back-pressure leads to additional grain refinement when the temperature remains constant [16, 33, 53] and, in addition, the presence of a back-pressure reduces the tendency for damage accumulation leading to billet cracking [49, 54].

An alternative procedure for achieving a homogeneous array of fine grains from an initial coarse grain structure is to conduct multiple-step ECAP processing in which the first passes are performed at a high temperature and the later passes at a lower temperature [21, 26, 38, 55]. This processing technique has similarities to using an extrusion step prior to ECAP because it refines the structure which then becomes the initial structure in the final processing.

An important direct consequence of the mechanism of grain refinement observed in magnesium alloys processed by ECAP is the potential for directly tailoring the grain size distribution. It is possible, for example, to control the area fractions of coarse and fine grains by changing the numbers of passes in ECAP [45, 46] and it is possible to control the final grain size by manipulating the processing parameters [29, 46]. The concept of grain boundary engineering was introduced many years ago to denote the potential for achieving beneficial material properties, such as high strength or good ductility, by manipulating the distributions of the grain boundary misorientations [56] and this approach was subsequently used for materials processed by ECAP [57, 58]. The present model suggests the alternative of grain size engineering where selected material properties may be achieved by manipulating the distributions of different grain sizes. This approach may be advantageous in, for example, producing a bi-modal distribution of grain sizes in order to give, as in earlier research on nanostructured copper [59], a combination of high strength and enhanced ductility in tensile testing at ambient temperature. The overall objective in this approach would be to use the ultrafine grains of the bi-modal distribution to achieve strength and the embedded larger grains to achieve a stability of the tensile deformation. Since bi-modal distributions are effective also in increasing ductility in cyclic deformation [60], fatigue testing may provide another opportunity for achieving improved properties by grain size engineering.

The effect of texture

The model developed in this report does not directly incorporate any texture effects into the process of grain refinement. Nevertheless, it is anticipated that the model will be valid for any initial texture and processing route. This general validity is anticipated because the mechanism of formation of the new grains along the original grain boundaries is observed in magnesium alloys having different initial textures when processing in the temperature range where ECAP is generally conducted. Consistent with this approach, a recent report compared the effect of texture in an AZ31 alloy processed by rolling and ECAP and concluded that texture has no effect on the size of the newly formed grains but rather it influences the extent of these new grains and the amount of deformation required to obtain their formation [61].

Summary and conclusions

1. Experiments on an AZ31 magnesium alloy show that processing by ECAP at 473 K produces a heterogeneous grain structure after two passes and a homogeneous

distribution of fine grains after six passes. The finer structure obtained by ECAP exhibits enhanced ductility at moderate temperatures.

2. A model is proposed for the grain refinement of magnesium alloys during processing by ECAP in the temperature range of ~420–600 K. This model is based on the principles of dynamic recrystallization in which necklace-like distributions of fine grains are nucleated along the grain boundaries and along twin boundaries.
3. The model for grain refinement is consistent with a wide range of experimental data and shows the potential for tailoring the distributions of grain sizes in magnesium alloys by controlling the processing parameters. This introduces the possibility of using grain size engineering to achieve selected material properties in magnesium alloys.

Acknowledgement This study was supported by the National Science Foundation of the United States under Grant No. DMR-0855009.

References

1. Valiev RZ, Langdon TG (2006) Prog Mater Sci 51:881
2. Xu C, Furukawa M, Horita Z, Langdon TG (2005) Mater Sci Eng A398:66
3. Langdon TG (2007) Mater Sci Eng A462:3
4. Kuhlmann-Wilsdorf D (1989) Mater Sci Eng A113:1
5. Kuhlmann-Wilsdorf D (1997) Scr Mater 36:173
6. Kawasaki M, Horita Z, Langdon TG (2009) Mater Sci Eng A524:143
7. Figueiredo RB, Langdon TG (2009) J Mater Sci 44:4758. doi:10.1007/s10853-009-3725-z
8. Iwahashi Y, Wang JT, Horita Z, Nemoto M, Langdon TG (1996) Scr Mater 35:143
9. Furukawa M, Iwahashi Y, Horita Z, Nemoto M, Langdon TG (1998) Mater Sci Eng A257:328
10. Figueiredo RB, Langdon TG (2008) J Mater Sci 43:7366. doi:10.1007/s10853-008-2846-0
11. Figueiredo RB, Langdon TG (2009) Mater Sci Eng A501:105
12. Figueiredo RB, Langdon TG (2009) Mater Sci Eng A503:141
13. Watanabe H, Takara A, Somekawa H, Mukai T, Higashi K (2005) Scr Mater 52:449
14. del Valle JA, Ruano OA (2007) Acta Mater 55:455
15. Langdon TG (2009) J Mater Sci 44:5998. doi:10.1007/s10853-009-3780-5
16. Lapovok R, Estrin Y, Popov MV, Langdon TG (2008) Adv Eng Mater 10:429
17. Ion SE, Humphreys FJ, White SH (1982) Acta Metall Mater 30:1909
18. Galiyev A, Kaibyshev R, Gottstein G (2001) Acta Mater 49:1199
19. Myshlyaev MM, McQueen HJ, Mwembela A, Konopleva E (2002) Mater Sci Eng A337:121
20. Beer AG, Barnett MR (2006) Mater Sci Eng A423:292
21. Ding SX, Chang CP, Kao PW (2009) Metall Mater Trans A 40A:415
22. Estrin Y, Yi SB, Brokmeier HG, Zúberová Z, Yoon SC, Kim HS, Hellmig RJ (2008) Int J Mater Res 99:50
23. Janeček M, Popov M, Krieger MG, Hellmig RJ, Estrin Y (2007) Mater Sci Eng A462:116
24. Koike J, Kobayashi T, Mukai T, Watanabe H, Suzuki M, Maruyama K, Higashi K (2003) Acta Mater 51:2055
25. Figueiredo RB, Langdon TG (2009) Int J Mater Res 100:1638
26. Kim HK, Kim WJ (2004) Mater Sci Eng A385:300
27. Su CW, Lu L, Lai MO (2006) Mater Sci Eng A434:227
28. Lin HK, Huang JC, Langdon TG (2005) Mater Sci Eng A402:250
29. Xia K, Wang JT, Wu X, Chen G, Gurvan M (2005) Mater Sci Eng A410:324
30. Jin L, Lin DL, Mao DL, Zeng XQ, Chen B (2006) Mater Sci Eng A423:247
31. Zúberová Z, Estrin Y, Lamark TT, Janeček M, Hellmig RJ, Krieger M (2007) J Mater Process Technol 184:294
32. Kang SH, Lee YS, Lee JH (2008) J Mater Process Technol 201:436
33. Xu C, Xia K, Langdon TG (2009) Mater Sci Eng A527:205
34. Kang F, Liu JQ, Wang JT, Zhao X (2009) Scr Mater 61:844
35. Miyahara Y, Horita Z, Langdon TG (2006) Mater Sci Eng A420:240
36. Mabuchi M, Ameyama K, Iwasaki H, Higashi K (1999) Acta Mater 47:2047
37. Máthis K, Gubicza J, Nam NH (2005) J Alloys Compd 394:194
38. Mussi A, Blandin JJ, Salvo L, Rauch EF (2006) Acta Mater 54:3801
39. Chen B, Lin DL, Jin L, Zeng XQ, Lu C (2008) Mater Sci Eng A483:113
40. Yamashita A, Horita Z, Langdon TG (2001) Mater Sci Eng A300:142
41. Suwas S, Gottstein G, Kumar R (2007) Mater Sci Eng A471:1
42. Gan WM, Zheng MY, Chang H, Wang XJ, Qiao XG, Wu K, Schwebke B, Brokmeier HG (2009) J Alloys Compd 470:256
43. Tang WN, Chen RS, Zhou J, Han EH (2009) Mater Sci Eng A499:404
44. Matsubara K, Miyahara Y, Horita Z, Langdon TG (2003) Acta Mater 51:3073
45. Ma AB, Jiang JH, Saito N, Shigematsu I, Yuan YC, Yang DH, Nishida Y (2009) Mater Sci Eng A513–A514:122
46. Lapovok R, Thomson PF, Cottam R, Estrin Y (2004) Mater Trans 45:2192
47. Lapovok R, Thomson PF, Cottam R, Estrin Y (2005) Mater Sci Eng A410:390
48. Watanabe H, Mukai T, Ishikawa K, Higashi K (2002) Scr Mater 46:851
49. Figueiredo RB, Cetlin PR, Langdon TG (2010) Metall Mater Trans A 41A:778
50. Horita Z, Matsubara K, Makii K, Langdon TG (2002) Scr Mater 47:255
51. Furui M, Kitamura H, Anada H, Langdon TG (2007) Acta Mater 55:1083
52. Figueiredo RB, Cetlin PR, Langdon TG (2007) Acta Mater 55:4769
53. Kang F, Liu JQ, Wang JT, Zhao X, Wu X, Xia K (2009) Int J Mater Res 100:1686
54. Lapovok RYe (2005) J Mater Sci 40:341. doi:10.1007/s10853-005-6088-0
55. Figueiredo RB, Langdon TG (2009) Scr Mater 61:84
56. Watanabe T (1984) Res Mech 11:47
57. Fujita T, Horita Z, Langdon TG (2004) Mater Sci Eng A371:241
58. Furukawa M, Horita Z, Langdon TG (2005) J Mater Sci 40:909. doi:10.1007/s10853-005-6509-0
59. Wang Y, Chen M, Zhou F, Ma E (2002) Nature 419:912
60. Mughrabi H, Höppel HW, Kautz M, Valiev RZ (2003) Z Metallkd 94:1079
61. del Valle JA, Ruano OA (2008) Mater Sci Eng A487:473